6. TSUNAMI

One of the most spectacular aspects of this earthquake was damage directly inflicted by a tsunami. This chapter describes the destructions caused by the tsunami. Dr. Koshimura (ERI, University of Tokyo, Tsunami), who joined the International Tsunami Survey Team (ITST 2001abc) reports their findings and his computer simulation of the tsunami surges in Sections 6.1 and 6.2, respectively. Dr. Hiroshi SATO (ERI, University of Tokyo, Surface geology), who surveyed La Punta area with the main party of the JSCE team, reports estimated wave heights and directions of tsunami surge at La Punta in Section 6.3.

6.1 POST TSUNAMI SURVEY

Introduction

The June 23 earthquake generated a destructive tsunami. It struck the Peruvian coast and was observed at tide gauges on the Peruvian coast and throughout the Pacific. The International Tsunami Survey Team (ITST 2001abc) , funded by National Science Foundation, surveyed the area affected by the tsunami. The main purpose of the trip was to examine the tsunami damage, measure the tsunami run-up height and extent of inundation, and interview the eyewitnesses of the event. The ITST consisted of nine scientists from the United States and Mexico. The ITST also collaborated with Peruvian scientists from the Direccion de Hidrografia y Navegacion of the Peruvian Navy. With the support of the Peruvian scientists, the trip was successful to collect the valuable knowledge from this event.

The ITST was deployed on the southern Peruvian coast from July 5 to 15, 2001. The surveyed route is indicated in **Figure 6.1**. It was found that the area affected by the tsunami extended along the coast of approximately 300 km, from Atico in the northwest to Ilo in the southwest. The following report aims to describe the findings and knowledge from the survey.

Figure 6.1 Survey route and area of the ITST effort deployed along the southern Peruvian coast

Tanaca / Chala

Tanaca / Chala area is at approximately 370 km south, driving from Lima on Pan American Highway. In Tanaca, there was no evidence indicating that this area was severely affected by the tsunami. However, the local eyewitnesses reported that the water receded shortly after the ground shaking and stayed for approximately 30 minutes, then came back to the level of normal high tide.

There was a small port and pier at Chala (see **Figure 6.2**). No significant damage was found on this facility. Eyewitnesses described that the water started receding immediately after the shaking and stopped its withdraw at 100 m offshore. Another fisherman reported that he did not see the sea bottom at the offshore end of the pier (approximately 180 m from the coast line) during the sea withdrawal.

Figure 6.2 Photo of the Pier of Chala

Atico

Two points were measured at Atico. One is based on the eyewitness account describing that the tsunami penetrated over the berm of the sandy beach and swept away the broken structures on its foundation. The measured tsunami height was 3 m (after tide correction) at the debris line shown by the eyewitness, which is 54 m inland from the shoreline.

Another point is a sort of uncertainty. There was a debris line behind the berm of the sandy beach that could be interpreted as the result of tsunami run-up. This debris line was found at 51 m inland from the shore line and it was the result of wave run-up overtopping the berm at the height of approximately 3.6 m above the sea level. The measured height of the debris line was 2.4 m (after tide correction). However, there was no eyewitness account at this point. So this point should be defined as ‘questionable’ for that reason, although the measured value is consistent with that of the previous point.

Ocona

Ocona is a town which locates very close to the earthquake epicenter. The measured tsunami run-up height was less than 3 m at the mouth of Ocona River. The Pan American Highway between Atico and Ocona was significantly damaged by the main shock and the aftershocks (see **Figure 6.3**).

Figure 6.3 Damaged Pan American Highway near Ocona

Camana

Camana is the town which was caused the most significant damage on the Peruvian coast. The damage in the municipality of Camana extended to 20 km long stretch of coastline. Over 2000 structures were damaged or destroyed and 2000 hectares of firmland were flooded. 22 people killed and 62 missing were reported. Besides, all of the casualties were because of the tsunami. The ITST spent 4 days in this area and measured the extent of tsunami inundation and run-up heights, and interviewed with the city, Red Cross officials and survivors.

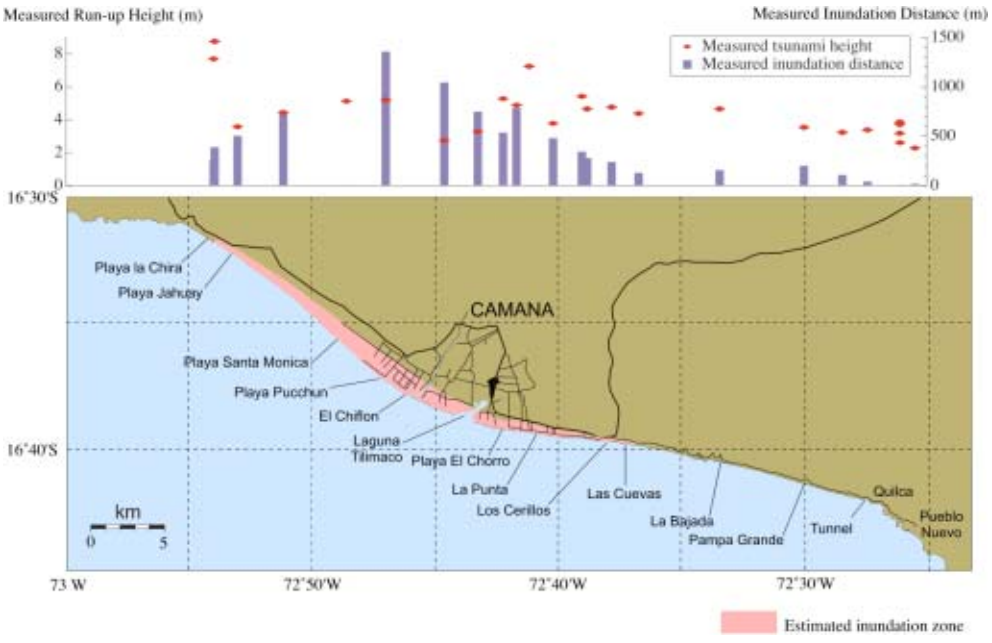

Figure 6.4 Measured run-up height and extent of inundation at Camana

Figure 6.4 indicates the distribution of tsunami run-up height and extent of inundation at Camana measured by the ITST. According to the eyewitness accounts, the tsunami arrived at Camana with strong leading depression followed by a series of positive waves. It was reported that four waves struck the coast of Camana and the second or third one was the largest. The average value of run-up heights was approximately 5 m. The sandy beach at Camana is very flat so that the tsunami could easily cause substantial inland penetration, typically 200 to 700 m and reached over 1 km at one location.

La Punta (see **Figure 6.4** for the location) was likely to be the most significantly affected by the tsunami. **Figure 6.5** is the photo showing the erosion of the beach of La Punta. The Pacific Ocean is at the right behind the road. The tsunami would penetrate through the beach from right to left, then the strong back wash current was occurred to cause the erosion. The maximum measured run-up height at La Punta was more than 7.25 m. **Figure 6.6** is the photo of the hotel building where the maximum run-up in La Punta was measured. The building was standing at approximately 70 m inland from the shoreline. Fortunately, the building withstood the wave force, though it was likely to be struck directly. Ws well as the other destroyed houses, scouring was occurred in front of the building.

Figure 6.5 The erosion of the beach of La Punta, Camana

Figure 6.6 Hotel building struck by the tsunami at La Punta

After the inspection at the site, it was found that construction method and quality would significantly affect the survival of the buildings. As shown in **Figure 6.7**, poorly built adobe and infilled wall structures were vulnerable for the impact of tsunami. The structures that survived the tsunami penetration appeared to have deeper foundations and more reinforcing.

Figure 6.7 Completely destroyed houses at La Punta

The western part of Camana district was mainly used as farmland, which was developed on the flat topography. At Playa Pucchun, the tsunami penetrated over the large area of the farmland as shown in **Figure 6.8**. The final tsunami trace (debris) was found at 1360 m inland from the shoreline. Further west of the developed farmland was the sandy beach. The maximum run-up in the entire region was measured as 8.8 m at Playa la Chira. As shown in **Figure 6.9**, the tsunami penetrated through the beach and ran up the steep slope.

Figure 6.8 Disturbed farmland at Playa Pucchun, Camana

Figure 6.9 Tsunami run-up on the steep slope at Playa la Chira

Casualties mainly consisted of farm workers and house keepers maintaining the beach houses during the winter season. While the wide extent of inundation and the number of destroyed structures, the number of lives lost was considerably less than other recent event, such as Papua New Guinea tsunami. The timing of the event was likely to reduce the loss of human lives. This event occurred in winter. The summer resident population of Camana beach would increase by 5000 people. If the earthquake had occurred in the summer when the beach and hotels were full, casualties could have been expected more.

Quilca

The town of Quilca, which is developed at the south-east of Camana, has a small harbor. In the town of Quilca, it was reported by the eyewitnesses that there were four distinct surges within the harbor. The tsunami arrived with withdrawal of water to the base of the fish loading dock at the bottom of the harbor. After the first withdrawal, the sea within the harbor oscillated several times. The tsunami penetration through the town was occurred after the third withdrawal of the water to reach up to 4 m above the sea level.

Mollendo

The beach of Mollendo, which locates approximately 90 km south-east of Camana. On the beach, the debris line was remained just behind the berm. The local resident reported that there was a withdrawal of water after the earthquake, however no positive wave. The resident also indicated that the water did not come over the berm on the day of tsunami. It was turned out the debris was the result of large swell occurred during the high tide after the earthquake. Thus, the tsunami height was not measured at this point.

Table 6.1 Summary of the tsunami impact along the southern Peruvian coast.

Place	Tsunami height	Feature / Impact
Tanaca / Chara	Not measured	Only the sea withdrawal shortly after the quake. / No tsunami damage.
Atico	3 m	Only the sea withdrawal shortly after the quake. / No tsunami damage.
Ocona	< 3 m	Only the sea withdrawal shortly after the quake. / No tsunami damage.
Camana	> 5 m	Initial sea withdrawal after the quake, the maximum run-up during 2nd or 3rd tsunami strike. / Destroyed over 2000 structures, flooded 2000 hectares of farmland, 22 killed and 62 missing.
Quilca	4 m	Initial sea withdrawal shortly after the quake. / Flooded the fishing facilities and town within the harbor.
Mollendo	Not measured	Only the sea withdrawal shortly after the quake. / No tsunami damage.
Ilo	Not measured	Only the sea withdrawal shortly after the quake. / No tsunami damage.

6.2 MODELING OF JUNE 23 PERUVIAN TSUNAMI

Introduction

The modeling effort of Peruvian tsunami was employed right after we received the information in terms of the seismic source parameters via the Internet. The widespread impact of this tsunami motivated the modeling efforts to produce a realistic simulation as soon as possible. The ITST has two resident numerical models, TUNAMI-N2 (Imamura 1995) and MOST (Titov and Synolakis 1998). Both models were used to produce preliminary simulation shortly after the earthquake, and the first results were posted on the Internet a day after the event [http://www.pmel.noaa.gov/tsunami/peru_pmel.html]. These numerical model results aimed to quantify the magnitude of the tsunami, to estimate the extent of impacted area and to guide the post-tsunami survey. The first simulations have been revised using new data in terms of the seismic source and the results of the post-tsunami survey by the International Tsunami Survey Team (ITST). The revised preliminary modeling results are indicated in the following and compared with the measured data by the ITST.

Modeling setup

TUNAMI-N2 model is used for modeling efforts focusing on the near-field tsunami propagation within the tsunami source region. In this model, a set of non-linear shallow water wave equations with bottom friction term are discretized by the leap-frog finite difference scheme.

For the modeling of tsunami propagation, we used the 2 minute digital bathymetry grid published by Smith and Sandwell (1997), available at [http://topex.ucsd.edu/marine_topo/mar_topo.html]. We re-sampled this grid and produced 1 minute grid (approximately 1744 m from west to east and 1845 m from north to south) for the propagation model. **Figure 6.10** shows the bathymetry of the computational domain.

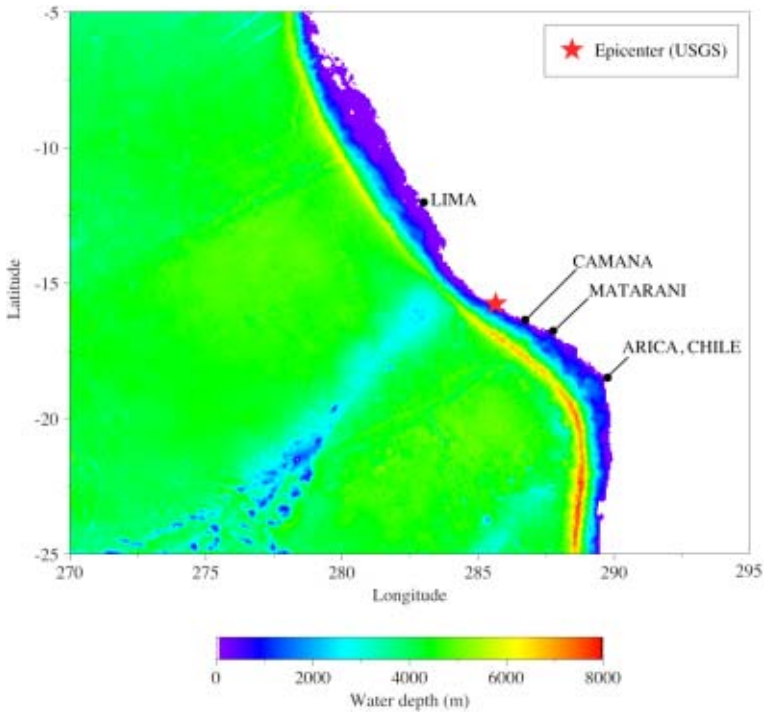

Figure 6.10 Bathymetry of the computational domain.

Tsunami source model

For the modeling of tsunami generation, we assume that the seismic deformation on the seafloor pushes up the overlying water instantaneously, that is, the feature of the sea bottom deformation reflects the initial water surface elevation. Here, we applied the theory of Okada (1985) to compute the

static seismic deformation.

The result of seismic deformation modeling is based on the recent seismic inversion results published by Kikuchi and Yamanaka (2001). Kikuchi and Yamanaka (2001) analyzed teleseismic broadband P waves retrieved from 24 stations and determined the general source parameters shown in **Table 6.2**.

Table 6.2 Generalized earthquake source parameters published by Kikuchi and Yamanaka (2001)

(Strike, Dip, Rake)	(309, 21, 61)
Depth	30 km
Seismic moment	2.2×10^{21} Nm

Also, they determined the moment release distribution in detail and slip angles on 40 fault segments within the rupture area of 150 km by 240 km. **Figure 6.11** shows the fault slip distribution within the rupture area, obtained from the results of Kikuchi and Yamanaka (2001). Each fault segment indicates the area of 30 km by 30 km. Large asperity is concentrated at approximately 150 km south from the initial break point (epicenter). However, because their analysis is based on the teleseismic waves, the estimate of the location of epicenter should be flexible, considering the observation of the local seismic deformations.

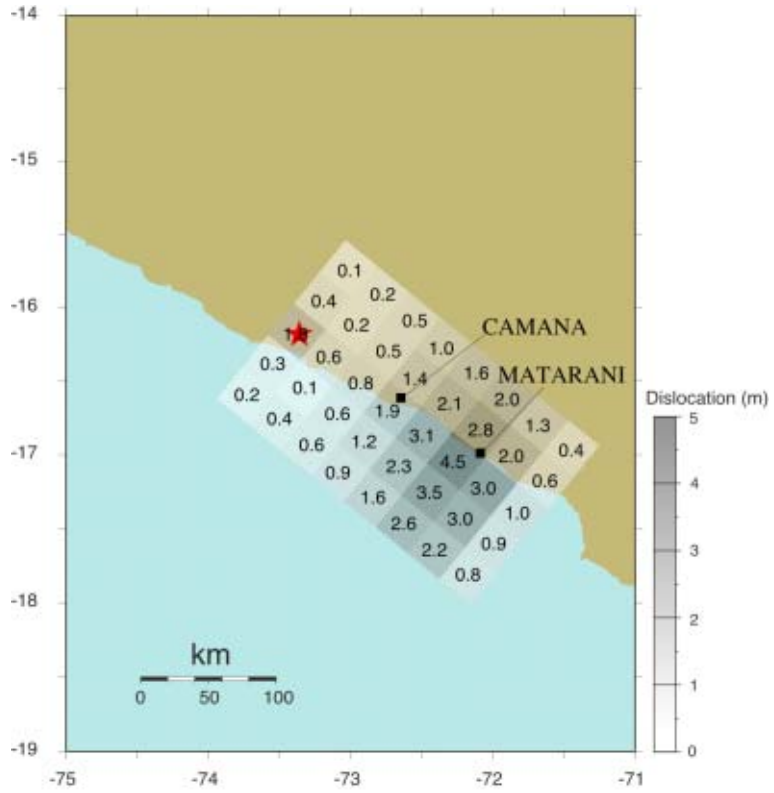

Figure 6.11 Fault slip distribution within the rupture area.

Here is a good example of tsunami record indicating the existence of local seismic deformation during the event. **Figure 6.12** shows the 1 hour-averaged tidal record at Matarani (Ortiz et al. 2001) and the mean sea level computed from the data. There is a discrepancy between the mean sea levels before and after the earthquake. The mean sea level rose approximately 15 cm after the tsunami struck. This sea level change indicates that the local subsidence was occurred during the earthquake.

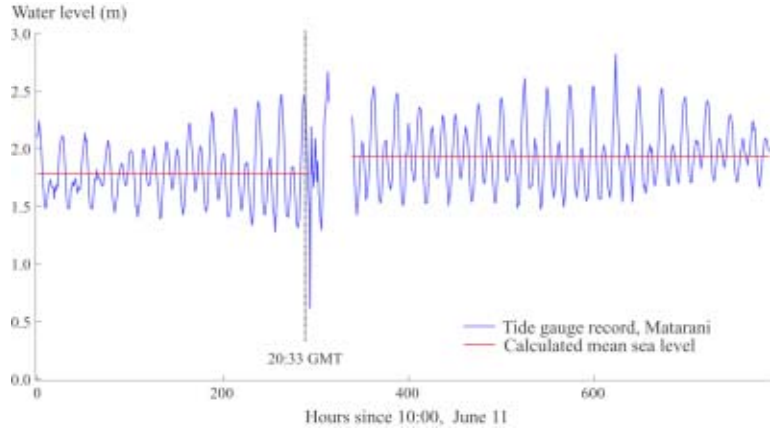

Figure 6.12 Sea level change at Matarani.

In order to be consistent with the observed subsidence at Matarani, we modified the position of the epicenter as 20 km northwest of the estimated epicenter of USGS. **Figure 6.13** is the computed seismic deformation based on the seismic inversion results of Kikuchi and Yamanaka (2001). However, there is still uncertainty on the location of the epicenter. We have not obtained any evidence indicating the co-seismic uplift at Camana.

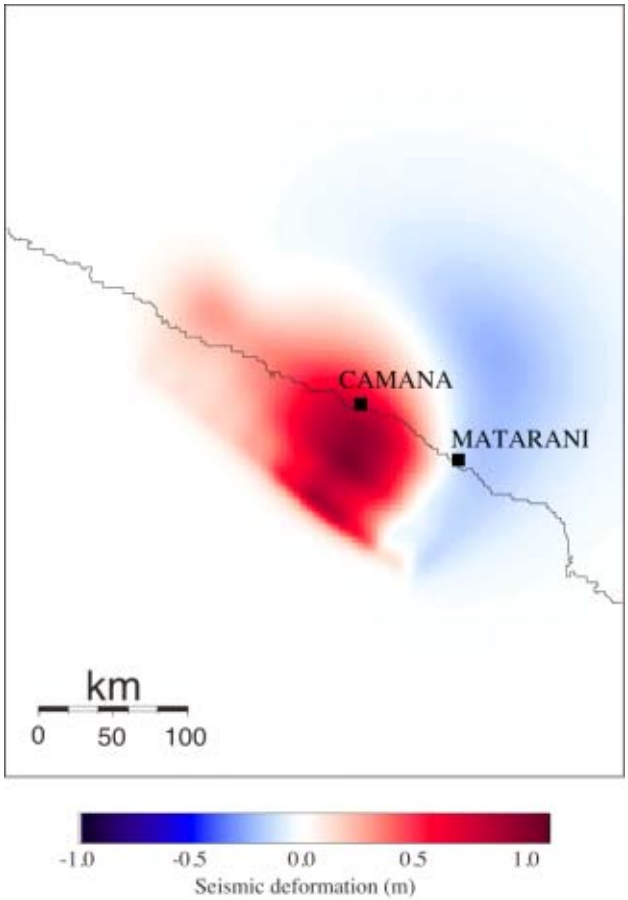

Figure 6.13 Computed seismic deformation.

Model results

Figure 6.14 indicates the comparison of computed maximum tsunami height and field measurements obtained by the ITST. Note that the computed tsunami height only reflects the offshore maximum water level of 30 m deep along the coast because of lack of the detailed bathymetry / topography data. Thus, the qualitative agreement between these two results in terms of the tsunami height should not be expected. However, the tsunami run-up profiles along the coast obtained from both results have good agreement. Both results indicate that tsunami energy is concentrated to the coast of Camana, which is approximately 50 km wide from west to east.

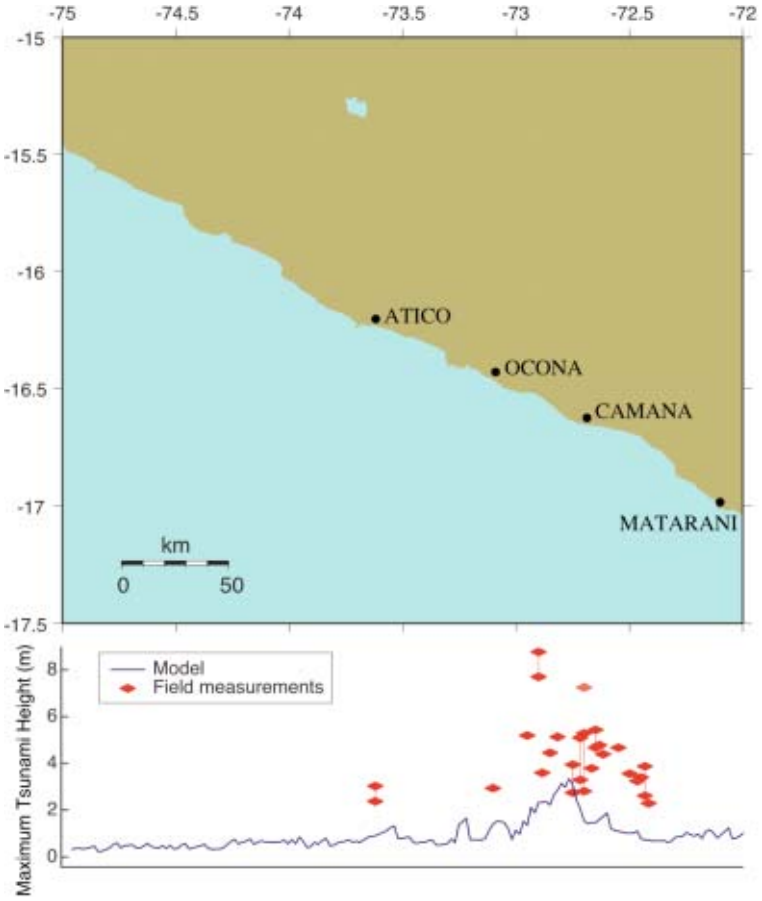

Figure 6.14 The comparison of computed maximum tsunami height with the measurement.

Figure 6.15 shows the computed tsunami waveforms at Camana, Matarani and Arica, Chile. In the diagram of Arica waveform, the model result is compared with the observed tsunami. The zero line of this diagrams is the mean sea level before the tsunami. Because Canama is included in the uplifted region, the initial sea level is estimated to be positive (above the mean sea level) shortly after the earthquake. The positive wave strikes Camana as the first arrival of tsunami. However, it doesn't exceed the amount of uplift of the land. This means that the significant positive wave as the first arrival of tsunami would not be recognized. Then, the water is receded and created negative wave. After that, the largest positive wave strikes the coast of Camana. This feature is consistent with the eyewitness accounts on the coast of Camana. Many of the witnesses described that "The water was receded after the quake and the strongest inundation occurred during the strike of second or third wave". The modeled and observed tsunamis at Arica indicate that the discrepancy exists in terms of the estimation of tsunami arrival time. The accuracy of estimated tsunami arrival time is affected by the estimate of tsunami source location (epicenter). Further discussion including determination of tsunami source location is necessary for the improvement of the model. Also, for more detailed

simulation such as the estimation of strong current and high frequency oscillation within the harbor as shown in the observed tsunami at Arica, more detailed bathymetry and topography data are required.

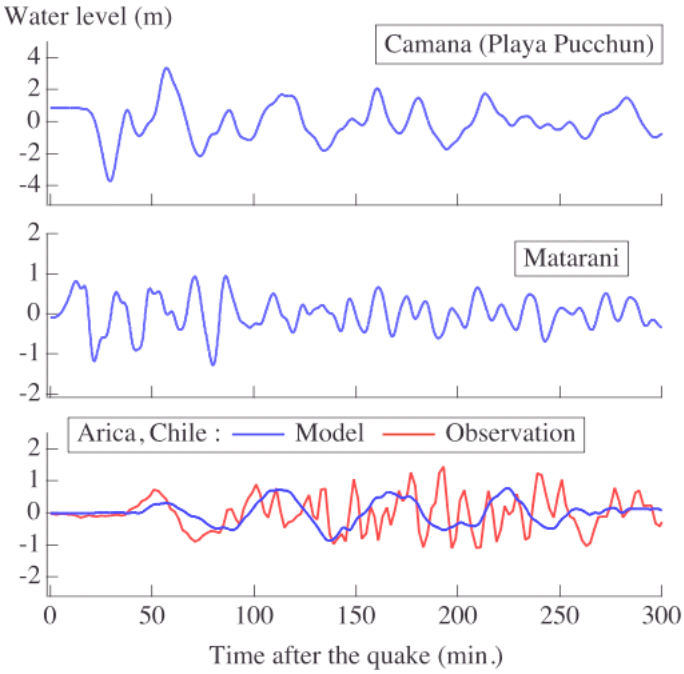

Figure 6.15 Computed and observed tsunami waveforms.

6.3 ESTIMATED WAVE HEIGHTS AND DIRECTION OF TSUNAMI SURGE AT LA PUNTA

As was described in Sections 6.1 and 6.2, Camana and its vicinity including La Punta located directly in the center of the affected coastline was the hardest hit zone. La Punta is a summer resort located along a narrow strip of beach with Los Cerrillos Hill rising behind. 26 people were reportedly killed by the tsunami, with roughly 70 still missing. Though tragic, this death toll was fairly light considering the location of the resort, because the tsunami occurred during the southern hemisphere winter. The orange colored zone in **Figure 6.16** is considered to have been inundated with water. The surges destroyed a great number of dwellings, hotels and restaurants there (**Figures 6.16**, **17** and **18**).

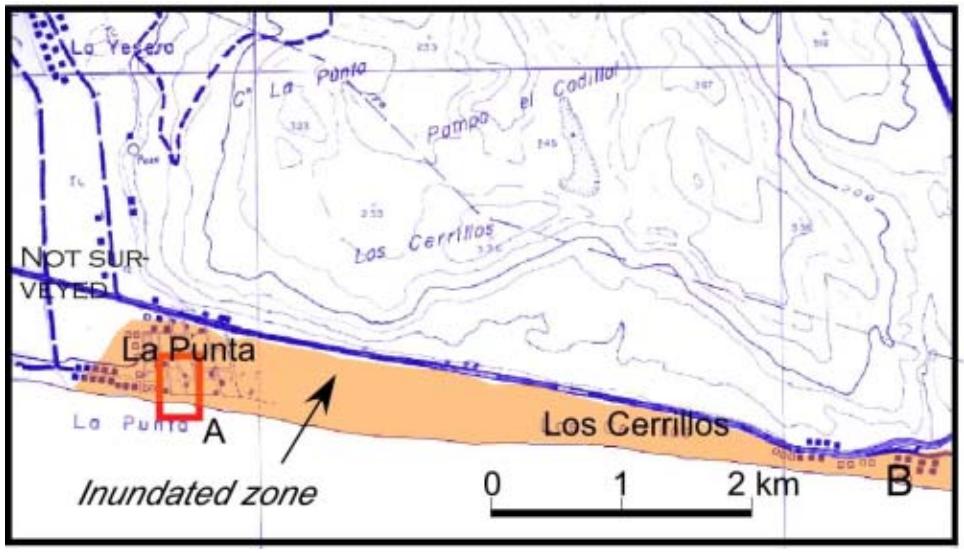

Figure 6.16 Inundated zone, La Punta

Figure 6.17 Destroyed dwellings by tsunami

Figure 6.18 A car caught in soft silty soils

Figure 6.19 Damage of houses in Los Cerrillios (Location B in **Figure 6.16**)

The inundated zone was covered thin with wet fine silty soils (**Figure 6.17**) suggesting that the water surged over the zone was stopped there for a while as is shown in **Figure 6.18**. The estimated height of tsunami is decreasing towards the land (**Figure 6.18**).

Figure 6.17 Sand layer, which derived by tsunami, is covered by thin silty soils.

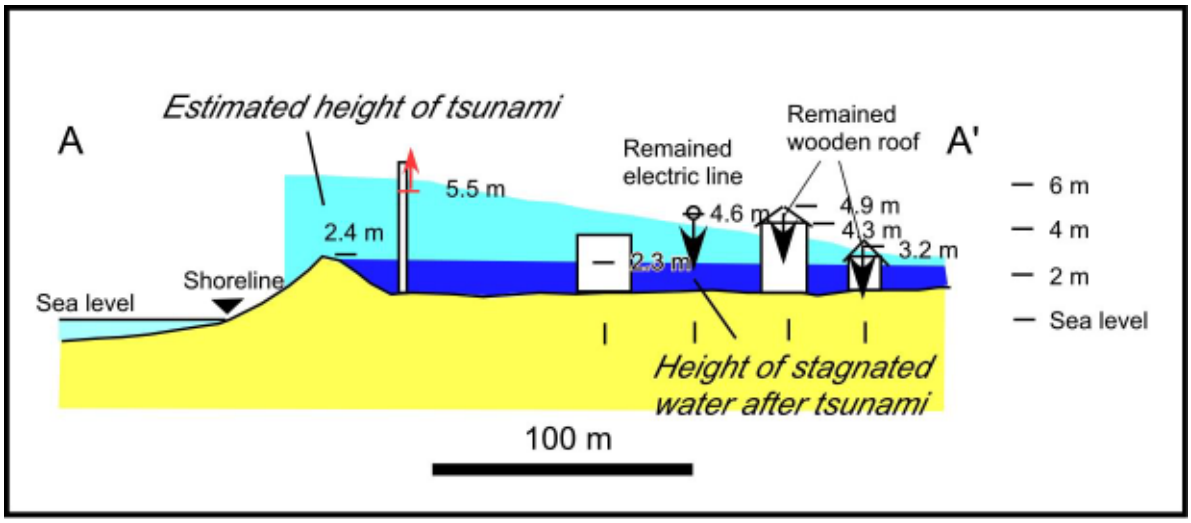

Figure 6.18 Cross sectional view of estimated height of tusnami. The location of the section is shown on **Figure 6.16**.

From a number of RC columns pushed down (**Figure 6.19**), possible directions of tsunami surges were estimated (**Figure 6.20**). Direction of the surge was also estimated from spalled utility poles (Figure 23). Two lines of utility poles along the coast were examined. Most poles on the front were still standing almost upright while those about 100m inland were more or less tilted because their foot soils were scoured by the surge. Probably for this reason, spalled poles were mostly found on the front. Lateral hair cracks were found on some poles, which seemingly suggest that the poles have experienced lateral shake before the area was inundated. The red arrows show inferred directions of strong ground motion, which seem to have been intense in about EW direction.

Figure 6.19 Reinforcing bars bent by tsunami.

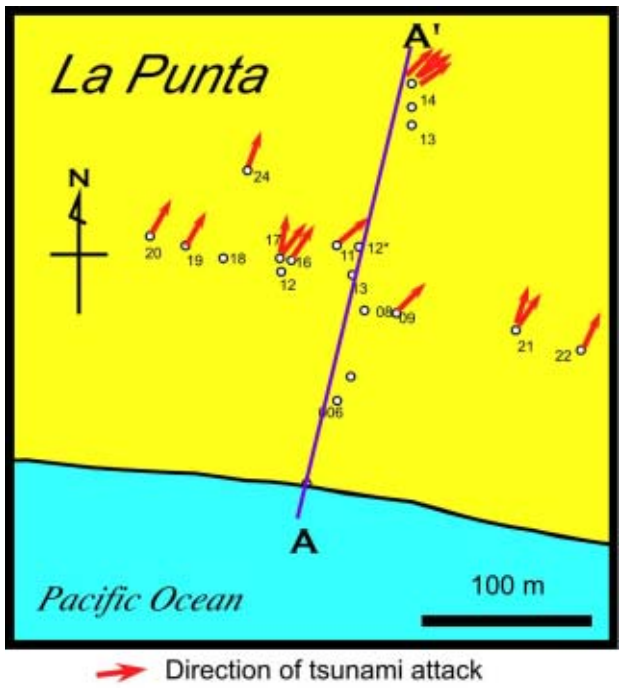

Figure 6.20 Possible directions of tsunami surge.

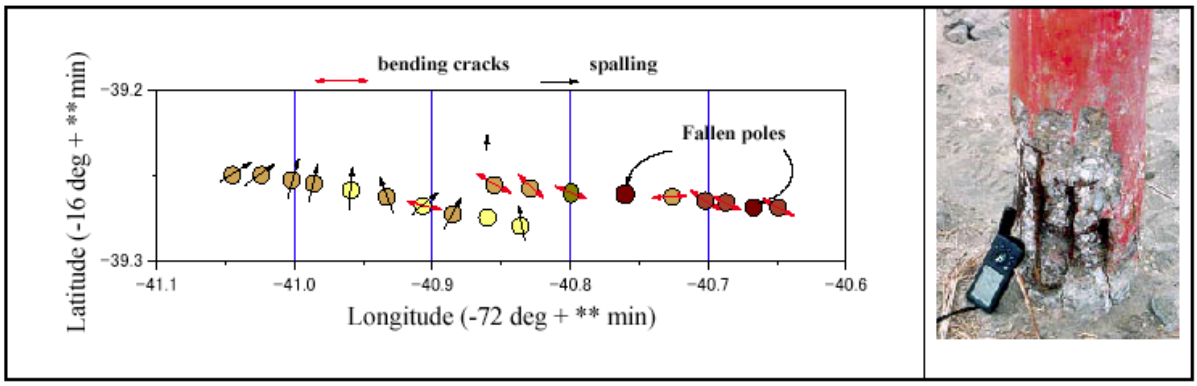

Figure 6.21 Spalled and cracked utility poles

6.4 SUMMARY

The ITST found that the damage due to the tsunami was mainly concentrated along the flat coastal beach of Camana, which is no higher than 5 m above the sea level. These developed beach would be significantly vulnerable. Poorly built adobe and infilled wall structures on the beach were heavily damaged by strong inundation current. Also the farmland developed on the flat beach were severely impacted. However, the timing of this event, occurring during mid-afternoon in winter, reduced the number of casualties. Also, initial draw down of water was the contributing cause of less casualties. The abnormal sight of receded sea water determined even the residents who were unaware of tsunamis to evacuate and go higher ground. The ITST findings are summarized in **Table 6.1**.

Numerical modeling of the June 23 Peruvian tsunami was performed with the latest tsunami source parameters provided by Kikuchi and Yamanaka (2001). The model results in terms of the tsunami height along the Peruvian coast explain the features of tsunami run-up along the Peruvian coast, that is, the tsunami energy concentration on the coast of Camana region of 50 km wide from west to east. However, there are discrepancies between the computed tsunami waveforms and the observations, especially about the tsunami arrival time. The estimate of the location of tsunami source should be considered as the future effort. For more detailed simulations of tsunami inundation on the land, strong current and oscillation within the harbor, more detailed bathymetry and topography data are necessary.

Possible direction of tsunami surges, deduced from the bent of reinforcing bars and spalling of utility poles, was from SSE to NNW at La Punta, Camana.

(**6.1, 6.2, 6.4**/ *Shunichi KOSHIMURA*, ERI, University of Tokyo)
(**6.3, 6.4**/ *Hiroshi SATO*, ERI, University of Tokyo)

ACKNOWLEDGEMENT
The hourly-recorded tide gauge data at Matarani was provided by Modesto Ortiz of CICESE, Mexico. Also, tide gauge data at Arica, Chile was provided by West Coast/Alaska Tsunami Warning Center through the Web-Link Compilation page of Pacific Marine Environmental Laboratory, NOAA [http://www.pmel.noaa.gov/tsunami/peru20010623.html].

REFERENCES

Imamura, F. (1995). *Review of tsunami simulation with a finite difference method*, long-wave runup models, World Scientific, 25-42.

ITST 2001 (2001a). *Report of the June 23, 2001 Peruvian Tsunami Field Survey of the International Tsunami Survey Team (ITST)* : Available from the ITST website: [http://www.usc.edu/dept/tsunamis/peru01/web%20pages/peru2001tsun.html]

ITST 2001 (2001b). *Impacts of the 2001 Peru Tsunami in Camana*, International Tsunami Symposium Proceedings, 409.

ITST 2001 (2001c). *The Peruvian tsunami of 23 June 2001 : Preliminary report by the International Tsunami Survey Team*, International Tsunami Symposium Proceedings, 377-378.

Kikuchi, M. and Y. Yamanaka, (2001). *Near Coast of Peru earthquake (Mw 8.2) on June 23, 2001*, EIC seismological note : **105** [http://wwweic.eri.u-tokyo.ac.jp/topics/200106232033/index.html]

Okada, Y. (1985). *Surface Deformation due to Shear and Tensile Faults in a Half-space*, Bulletin of the Seismological Society of America, **75**, **4**, 1135-1154.

Ortiz, M., G. Laos, D. Olcese and F. Vegas (2001). *Preliminary analysis of the June 23, 2001 Peru tsunami as recorded by two tide gauges in Matarani*, Draft of report.

Smith, W. H. F., and D. T. Sandwell (1997). *Global Sea Floor Topography from Satellite Altimetry and Ship Depth Soundings*, Science, **277**, 1956-1962.

Titov, V. V. and Synolakis, C. E., (1998). *Numerical modeling of tidal wave runup*, Journal of Waterways, Ports, Coastal and Ocean Engineering, **124 (4)**, 157-171.

to the next page